

A Passive Three-Phase Rectifier with High Power Factor

Deivis Borgonovo and Ivo Barbi

Federal University of Santa Catarina

Department of Electrical Engineering – Power Electronics Institute

E-mail: deivis@inep.ufsc.br, ivobarbi@inep.ufsc.br

Abstract – This paper presents a passive three-phase high-power-factor rectifier, with low THD of the input currents, using capacitors and inductors in the input side, without output low-frequency filtering inductor. The structure is very simple and robust, being recommended for applications where low THD and no high-frequency components are necessary. Its performance is considered optimal for AC-systems with high frequency, like on board appliances, what reduces the size of passive elements proportionally. The converter, the relevant topological stages, a mathematical analysis, design procedure and finally simulation and experimental results are presented, for an output power of 3.6kW.

I. INTRODUCTION

It is well known that the electrical energy is commercially available as alternating current (AC). However, for several applications, specially for electronic equipments, the direct current (DC) is more suitable. Therefore AC-to-DC converters, i.e. rectifiers, are used to convert the energy commercially available to a form that can be effectively used by these equipments. Furthermore, for high power levels, usually over some kilowatts, three-phase converters are used to assure power balance among the three phases.

Conventional three-phase rectifiers, using diodes and/or thyristors, show undesirable input characteristics, causing problems for the grid such as:

- High harmonic distortion and displacement at the line currents, causing low power factor and high levels of reactive power, increasing the costs of the whole system;
- Harmonic distortion at the grid voltage waveform and losses at the transmission lines, due to the current harmonic components flowing through the line impedances;
- Electromagnetic interference (EMI), that may cause problems in some susceptible equipments, just as control or communication systems.

The development of three-phase rectifiers, with high power factor and low current THD is attractive due the inconveniences listed above. The PWM three-phase rectifiers present some power limitations due to technology of the semiconductor devices. Furthermore, they present high cost, increased complexity and low robustness compared to passive converters.

For high power levels, or when robustness and/or low costs and complexity are desired, with high power factor and low harmonic distortion at the line currents, the passive three-phase rectifiers with high power factor consist in a quite attractive solution.

II. THE PROPOSED TOPOLOGY AND TOPOLOGICAL STAGES

The proposed topology for the passive three-phase rectifier, with high power factor, is presented in Fig. 1.

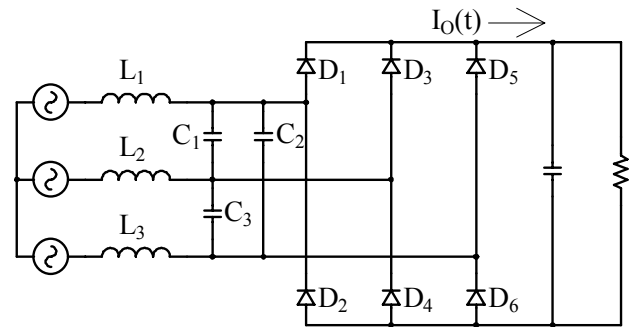
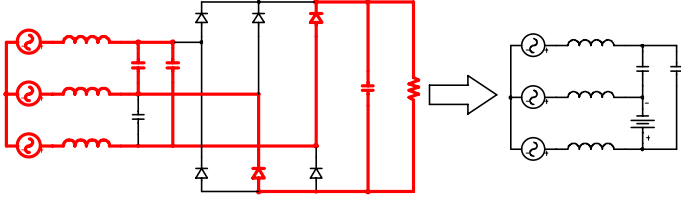


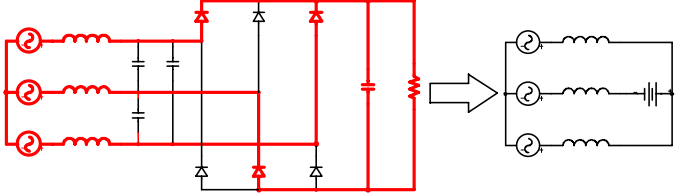
Fig. 1 – Proposed topology of the passive three-phase rectifier.

It must be observed that the structure is not a LC filter associated to a diode bridge, because they do not operate as independent structures, but interact between themselves constituting a single nonlinear structure. The accurate design of this circuit provides nearly sinusoidal input currents, resulting in twelve topological stages. Due to the inherent symmetry, only the first six stages and relevant waveforms will be presented, according to Fig. 2, for $0^\circ < \alpha < 180^\circ$.

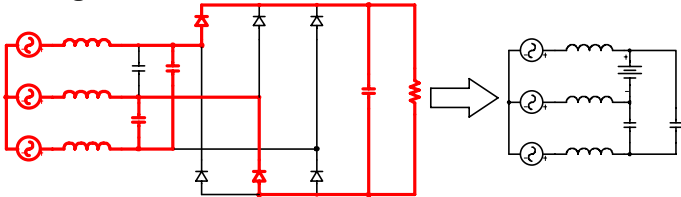
1st stage: $t_0 < \omega t < t_1$



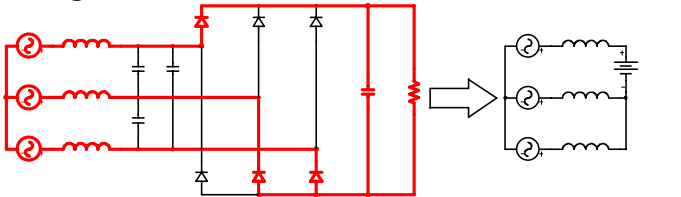
2nd stage: $t_1 < \omega t < t_2$



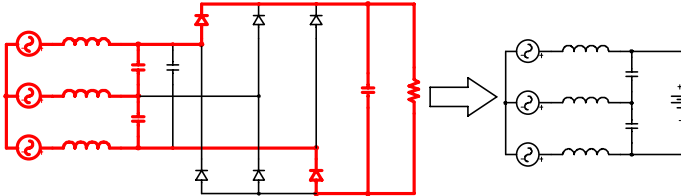
3rd stage: $t_2 < \omega t < t_3$



4th stage: $t_3 < \omega t < t_4$



5th stage: $t_4 < \omega t < t_5$



6th stage: $t_5 < \omega t < t_6$

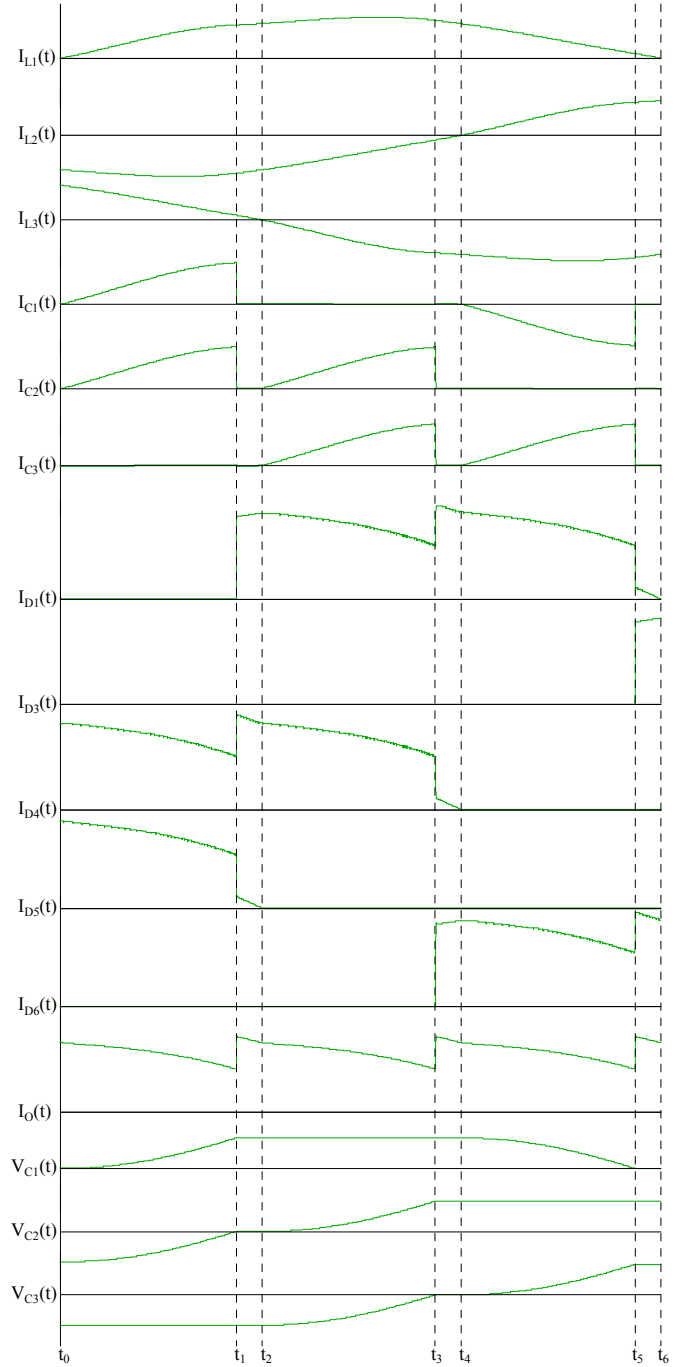
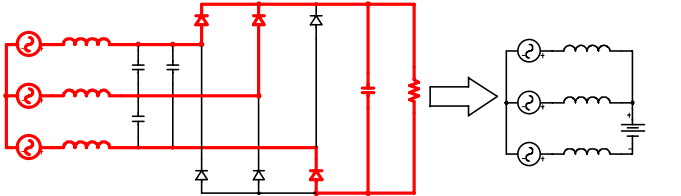


Fig.2: Topological stages and basic waveforms, for $0^\circ < \omega t < 180^\circ$.

For the analysis, it is assumed that $L_1=L_2=L_3$ and $C_1=C_2=C_3$. Observing the topological stages, it is simple to identify only two distinct basic stages (1st and 2nd, 3rd and 4th and so on), as the remaining ones are symmetrical between themselves. There are six sub-stages, where each one is symmetrical to the others and presents necessarily the same time interval, that obviously corresponds to a 60°

sector, as a complete cycle comprehends 360° .

Such symmetry simplifies the analysis, since the results obtained from one sub-stage can be extended to the remaining ones.

III. MATHEMATICAL ANALYSIS

Due to the symmetry of 60° among the sub-stages, as mentioned above, it is only necessary to study and analyze a single sub-stage. A given sub-stage is chosen, and in this case, for simplicity, the one comprehended between $t_0 < \omega t < t_2$. It is also assumed that $L_1=L_2=L_3$ and $C_1=C_2=C_3$. The supply voltages are balanced and defined as:

$$\begin{aligned} V_1(t) &= V_p \cdot \sin(\omega \cdot t) \\ V_2(t) &= V_p \cdot \sin(\omega \cdot t - 120^\circ) \\ V_3(t) &= V_p \cdot \sin(\omega \cdot t + 120^\circ) \end{aligned} \quad (1)$$

Hence from the first operating stage shown in Fig. 2, it gives:

$$\begin{cases} I_{L1}(t) + I_{L2}(t) + I_{L3}(t) = 0 \\ [V_1(t) - V_2(t)] = L \cdot \left[\frac{dI_{L1}(t)}{dt} - \frac{dI_{L2}(t)}{dt} \right] + V_{C1}(t) \\ [V_2(t) - V_3(t)] = L \cdot \left[\frac{dI_{L2}(t)}{dt} - \frac{dI_{L3}(t)}{dt} \right] - V_O \end{cases} \quad (2)$$

As the sum of the currents is null, since there is no neutral connection, the sinusoidal waveform and null phase displacement must be assured for two phases only. It is also convenient to define the expression of $V_{C1}(t)$, because it defines the end of the first operating stage.

Solving the respective differential equations, it provides:

$$I_{L1}(t) = \frac{V_p}{Z} \cdot \left\{ \frac{3 \cdot a}{(a^2 - 1)} \cdot \left\{ \cos(\omega \cdot t_0) \cdot [\cos(\omega \cdot t) - \cos(a \cdot \omega \cdot t)] \right\} + \sin(\omega \cdot t_0) \cdot [a \cdot \sin(a \cdot \omega \cdot t) - \sin(\omega \cdot t)] \right\} + \left\{ b \cdot \sin(a \cdot \omega \cdot t) + \frac{2 \cdot P_o \cdot Z \cdot \sin(\omega \cdot t_0)}{3 \cdot \eta \cdot V_p^2} \cdot \cos(a \cdot \omega \cdot t) \right\} \quad (3)$$

$$I_{L3}(t) = \left\{ I_p \cdot \sin\left(\frac{2 \cdot \pi}{3} + \omega \cdot t_0\right) + \frac{1}{2} \cdot [I_{L1}(t_0) - I_{L1}(t)] + \frac{3 \cdot a \cdot V_p}{2 \cdot Z} \cdot [\sqrt{3} \cdot [\sin(\omega \cdot t + \omega \cdot t_0) - \sin(\omega \cdot t_0)] - b \cdot \omega \cdot t] \right\} \quad (4)$$

$$V_{C1}(t) = \frac{V_p}{2} \cdot \left\{ \frac{3 \cdot a}{(a^2 - 1)} \cdot \left\{ \cos(\omega \cdot t_0) \cdot [a \cdot \sin(\omega \cdot t) - \sin(a \cdot \omega \cdot t)] \right\} + \sin(\omega \cdot t_0) \cdot [a \cdot \cos(\omega \cdot t) - a \cdot \cos(a \cdot \omega \cdot t)] \right\} + \left\{ b \cdot [1 - \cos(a \cdot \omega \cdot t)] + \frac{2 \cdot P_o \cdot Z \cdot \sin(\omega \cdot t_0)}{3 \cdot \eta \cdot V_p^2} \cdot \sin(a \cdot \omega \cdot t) \right\} \quad (5)$$

As shown Fig. 2, from the second stage, it can be written:

$$\begin{cases} V_1(t) - V_2(t) = L \cdot \frac{dI_{L1}(t)}{dt} - L \cdot \frac{dI_{L2}(t)}{dt} + V_O \\ V_1(t) - V_3(t) = L \cdot \frac{dI_{L1}(t)}{dt} - L \cdot \frac{dI_{L3}(t)}{dt} \\ I_{L1}(t) + I_{L2}(t) + I_{L3}(t) = 0 \end{cases} \quad (6)$$

Solving the respective differential equations, it provides:

$$I_{L1}(t) = \left[I_{L1}(t_1) + \frac{a \cdot V_p}{Z} \cdot \left\{ 3 \cdot \left[\cos(\omega \cdot t_1) - \cos(\omega \cdot t + \omega \cdot t_1) \right] - b \cdot \omega \cdot t \right\} \right] \quad (7)$$

$$I_{L3}(t) = I_{L3}(t_1) + \frac{a \cdot V_p}{Z} \cdot \left\{ 3 \cdot \left[\cos(\omega \cdot t_1) - \cos(\omega \cdot t + \omega \cdot t_1) \right] + 3 \cdot \sqrt{3} \cdot \left[\cos\left(\omega \cdot t + \omega \cdot t_1 + \frac{10 \cdot \pi}{12}\right) - \cos\left(\omega \cdot t_1 + \frac{10 \cdot \pi}{12}\right) \right] - b \cdot \omega \cdot t \right\} \quad (8)$$

where:

ω – power grid frequency [rad/s];
 V_p – peak input voltage;
 P_o – output power;
 η – overall efficiency of the converter.

And:

$$Z = \sqrt{\frac{3 \cdot L}{C}} \quad (9)$$

$$\omega_x = \frac{1}{\sqrt{3 \cdot L \cdot C}} \quad (10)$$

$$a = \frac{\omega_x}{\omega} \quad (11)$$

$$b = \frac{V_o}{V_p} \quad (12)$$

Therefore, it results:

$$L = \frac{Z}{3 \cdot a \cdot \omega} \quad (13)$$

$$C = \frac{1}{Z \cdot a \cdot \omega} \quad (14)$$

It must be mentioned that, in the second stage, the voltages on the capacitors remain constant. It is also known that the time intervals concerning both stages correspond to a 60° sector of the supply voltages full cycles, i.e.:

$$(t_1 - t_0) + (t_2 - t_1) = (t_2 - t_0) = \Delta t \quad (15)$$

$$\omega \cdot \Delta t = 60^\circ \quad (16)$$

$$\Delta t = \frac{2 \cdot \pi}{\omega} \cdot \frac{60^\circ}{360^\circ} \quad (17)$$

Considering that the supply voltages are purely sinusoidal, it can be said that the active power can be calculated employing only the fundamental component of the input current in each phase. As a null phase displacement among the supply voltages and the input currents in the phases is desired, the respective fundamental components are given as:

$$\begin{cases} I_{L1}(t) = I_p \cdot \sin(\omega \cdot t) \\ I_{L2}(t) = I_p \cdot \sin(\omega \cdot t - 120^\circ) \\ I_{L3}(t) = I_p \cdot \sin(\omega \cdot t + 120^\circ) \end{cases} \quad (18)$$

$$\text{where } I_p = \frac{2 \cdot P_o}{3 \cdot \eta \cdot V_p}$$

If the elements of the converter are designed adequately, the time intervals that define 60° can be controlled, and variable D is defined as:

$$\begin{cases} (t_1 - t_0) = D \cdot \Delta t \\ (t_2 - t_1) = (1 - D) \cdot \Delta t \end{cases} \quad (19)$$

Besides that, t_0 corresponds to the displacement among the voltage on the capacitors and the currents in the inductors.

Therefore, in order to assure the null phase among currents and voltages, the elements of the converter must be designed so that the following conditions are established.

If

$$\begin{cases} I_{L1}(t0) = I_p \cdot \sin(\omega \cdot t0) \\ I_{L3}(t0) = I_p \cdot \sin(\omega \cdot t0 + 120) \\ V_{C1}(t0) = 0 \end{cases} \quad (20)$$

Then

$$\begin{cases} I_{L1}(t2) = I_p \cdot \sin(\omega \cdot t2) \\ I_{L3}(t2) = I_p \cdot \sin(\omega \cdot t2 + 120) \\ V_{C1}(t1) = V_o \end{cases} \quad (21)$$

Or, in another words,

$$\begin{cases} I_{L1}(\Delta t) = I_p \cdot \sin(\omega \cdot \Delta t) \\ I_{L3}(\Delta t) = I_p \cdot \sin(\omega \cdot \Delta t + 120) \\ V_{C1}(D \cdot \Delta t) = b \cdot V_p \end{cases} \quad (22)$$

It means that, at the beginning of the period, it is considered that the currents maintain the desired value, and the elements are designed so that, at the end of the respective sector, such currents maintain the desired values at that instant.

Therefore, it is assured that, in steady state operation, if sector 1 maintains the currents in the desired values, they will be maintained constant and applied to sector 2. Since both them are symmetrical, the values will be maintained

in sector 3 as well, and so on. At last, sector 6 applies the accurate values to sector 1, as the assumption made above is valid, and a full cycle is completed.

Besides that, as mentioned before, there is no neutral connection, and the desired forms are only necessary to two of the three phases.

The analytical solution of the expressions developed above will not be presented here, because they are too extensive. However, it must be mentioned that, if a value is provided to one of the parameters, i.e. P_o , D , $t0$, a , b or Z , the remaining ones can be determined.

Thanks to the existent symmetry, the mathematical analysis could be developed for a sub-stage of 60° , and then extended to the complete period of 360° .

For a given

ω – power grid frequency [rad/s];

$V_p \rightarrow$ peak input voltage;

V_o – output voltage;

P_o – output power [kW];

η – overall efficiency of the converter.

ω_x – resonant frequency of the input filter.

the following expression set results.

$$\begin{aligned} Z &= \sqrt{\frac{3 \cdot L}{C}} & a &= \frac{\omega_x}{\omega} & L &= \frac{Z}{3 \cdot a \cdot \omega} \\ \omega_x &= \frac{1}{\sqrt{3 \cdot L \cdot C}} & b &= \frac{V_o}{V_p} & C &= \frac{1}{Z \cdot a \cdot \omega} \end{aligned}$$

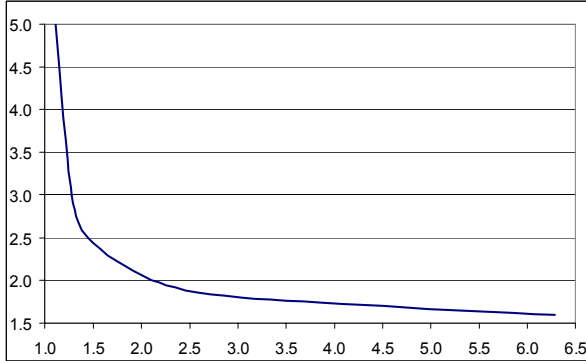


Fig. 3 – Parametrical curve: $b \times a$.

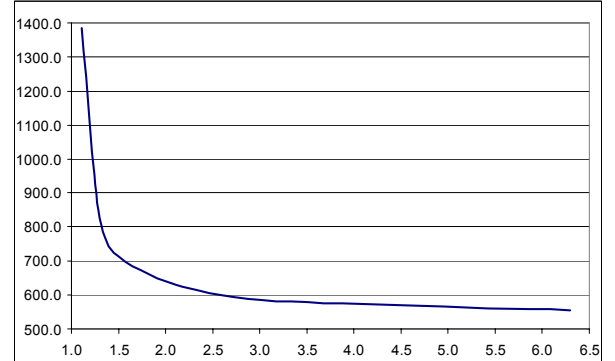


Fig. 4 – Parametrical curve: $P_o \cdot Z \times a$.

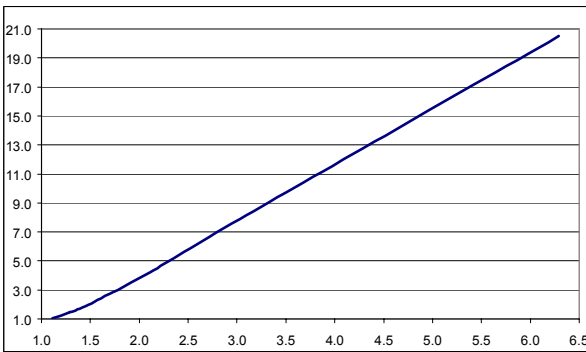


Fig. 5 – Parametrical curve: current THD $\times a$.

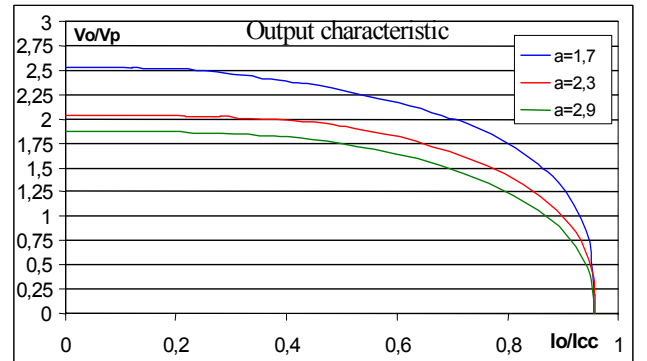


Fig. 6 – Output characteristic.

Fig. 3 shows that parameters a and b are directly related between themselves and independent on Z and P_o , so when a tends to unity, b tends to infinite. Observing Fig. 5, when a tends to unity, the current THD ideally tends to zero. Therefore, theoretically speaking, the current THD can be chosen, and a and

b are obtained from the graphs. Defining P_o and using the graph shown in Fig.4, Z can be determined. If parameters a , b and Z are known, V_o , L and C can be calculated.

IV. DESIGN EXAMPLE

Step 1	Step 2	Step 3	Step 4
Design specifications	Calculated	Obtained from the graphics	Calculated
$f = 60\text{Hz}$ $V_p = 311\text{V}$ $V_o = 600\text{V}$ $P_o = 3.6\text{kW}$	$w = 377$ $b = 1.93$	$a = 2.35$ $Z = 170$ $\text{THD} = 5\%$	$L = 64\text{mH}$ $C = 6.6\mu\text{F}$

V. SIMULATION AND EXPERIMENTAL RESULTS

Simulation results were obtained from software Pspice, according to the design example presented in section IV.

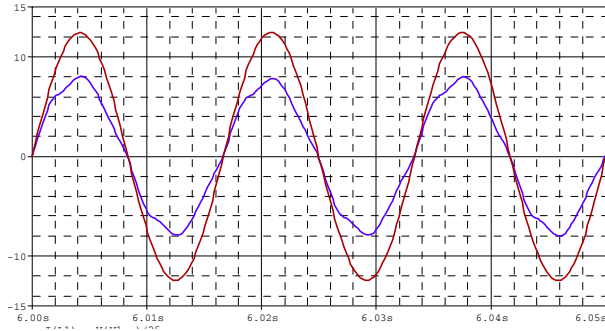


Fig. 7 – Voltage and input current in phase 1, obtained from simulation.

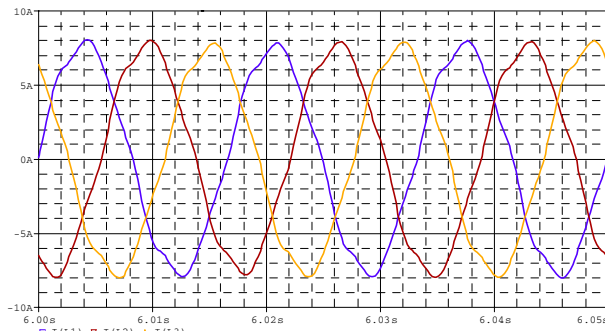


Fig. 9 – Input currents, obtained from simulation.

Experimental results were obtained from a prototype of 3.6kW, according to the design example presented in section IV.

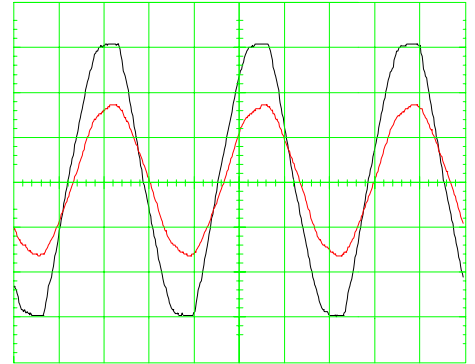


Fig. 8 – Voltage and input current in phase 1, obtained from the prototype.

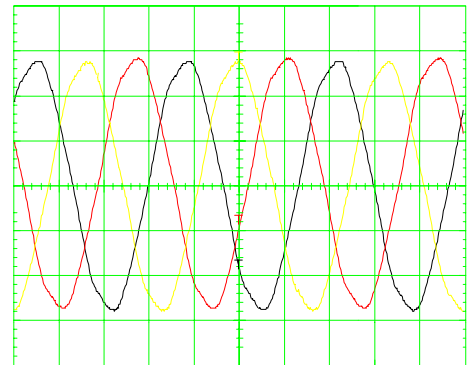


Fig. 10 – Input currents, obtained from the prototype.

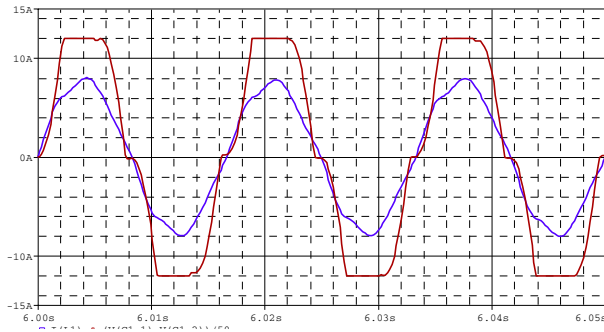


Fig. 11 – Input current in phase 1 and voltage on capacitor C_1 , obtained from simulation.

$V_o = 599V$
Voltage THD = 0%
Current THD = 5%
Displacement power factor (ϕ) = 4°
 $\cos(\phi) = 0.997$
Power factor = 0.996

VI. CONCLUSION

A new topology for a passive three-phase rectifier has been presented, with high power factor and low current THD. The experimental results shows that the current THD is lower than the supply voltage THD. An unexpected displacement factor has also been verified, due to the line inductance and the auto-transformer used to regulate the supply voltages.

The passive elements presented high weight and volume, but in fact this converter is recommended for high power levels, especially when there is low load variation, being also suitable for operation with high frequency voltage sources, like on board appliances. For example, for a given frequency of 400Hz and an output power of 100kW, with $V_o = 2V_P$, and using the graphs presented above, it provides $L = 430\mu H$ and $C = 27\mu F$. Simulation tests with such parameters have provided a current THD equal to 4.4%, with a power factor of 0.998.

The main advantages of the proposed topology lie

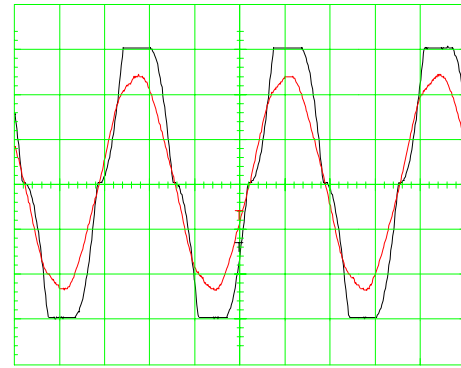


Fig. 12 – Input current in phase 1 and voltage on capacitor C_1 , obtained from the prototype.

$V_o = 605V$
Voltage THD = 4%
Current THD = 2.9%
Displacement power factor (ϕ) = 12° (due to line inductance from the “varivolt”
 $\cos(\phi) = 0.978$
Power Factor = 0.976

in the simplicity and easy implementation, low cost and extremely low current THD, for a passive converter, even lower than the voltage sources THD rates of the analyzed prototype.

REFERENCES

- [1] INSTITUTE OF ELECTRICAL AND ELECTRONICS ENGINEERS: IEEE-519. Recommended Practices and Requirements for Harmonic Control in Electric Power Systems, 1992.
- [2] Barbi, I ”Eletrônica de Potência”. Florianópolis. Editora da UFSC, 1986.
- [3] Seixas, F. J. M. S., “Conversores CA-CC de 12kW com Elevado Fator de Potência Utilizando Autotransformador com Conexão Diferencial de Múltiplos Pulsos”. PhD Tesis, INEP-UFSC, Florianópolis, 2001.
- [4] D. Borgonovo, “Modelagem e Controle de Retificadores PWM Trifásicos Empregando a Transformação de Park”, Master’s Degree Dissertation, INEP/EEL/UFSC, November/2001.